2009

# Mathematical Model of the Chronic Lymphocytic Leukemia Microenvironment

Ben Fogelson
*Harvey Mudd College*

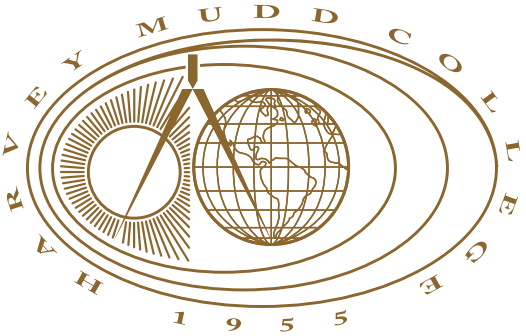


# Mathematical Model of the Chronic Lymphocytic Leukemia Microenvironment

**Ben Fogelson**

Lisette dePillis, Advisor

Rachel Levy, Reader

May, 2009

HARVEY MUDD COLLEGE

Department of Mathematics

# Abstract

A mathematical model of the interaction between chronic lymphocytic leukemia (CLL) and CD4+ (helper) T cells was developed to study the role of T cells in cancer survival. In particular, a system of four nonlinear advection-diffusion-reaction partial differential equations were used to simulate spatial effects such as chemical diffusion and chemotaxis on CLL survival and proliferation.

# Contents

# List of Figures

# List of Tables

# Acknowledgments

I would like to thank my research advisor, Lisette dePillis, and my second reader, Rachel Levy. I would also like to thank Claire Connelly, Darryl Yong, Ali Nadim, Aaron Fogelson, and Amy Chow for their useful conversations and suggestions.

My thanks also to John Milton and the REBMI (Research Experiences at the Biology–Mathematics Interface) program for support of the early stages of this research.

# Chapter 1

# Biological Background

B-cell chronic lymphocytic leukemia (CLL) is an incurable cancer and is the most common leukemia in the western world (Caligaris-Cappio and Dalla-Favera, 2005), constituting nearly 31% of all cases of human leukemia in patients over 50 years old (Martinis et al., 2005) with an estimated 15,110 new cases in the United States in 2008 (National Cancer Institute). The disease seldom occurs in people under 40 years of age (Vitale et al., 2003).

CLL is a cancer of the immune system, and is characterized by the uncontrolled growth of B lymphocytes (B cells), one of the main types of immune system cells. While B-cell growth is necessary for a healthy immune system (Abbas and Lichtman, 2005), the unchecked proliferation of B cells typical of CLL can cause the immune system, the circulatory system, the bone marrow, and other vital bodily networks to malfunction. Eventually, these breakdowns result in death.

Despite the fact that CLL is eventually fatal, the rate at which the cancer progresses varies greatly between individual patients. The disease can be roughly divided into two forms: a fast-progressing pathway and a slow-progressing pathway. Those with the slow-progressing pathway may not require treatment for many years (Vitale et al., 2003; Messmer et al., 2005), whereas those with the fast-progressing pathway can die in spite of treatment within a year of diagnosis (Vitale et al., 2003).

CLL is obviously a clinically important disease, but many features of the disease are still poorly understood. In particular, researchers have encountered extreme difficulties in keeping the malignant B cells alive in vitro (Caligaris-Cappio and Dalla-Favera, 2005), which is not the case for most cancer cell lines. The in vitro mortality of CLL cells suggests that other signals or forces inside the body must be responsible for keeping CLL alive

in vivo.

Recent biological research (see, e.g., Ghia et al., 2002; Caligaris-Cappio and Dalla-Favera, 2005) suggests that T lymphocytes (T cells), which are also immune system cells, are capable of promoting CLL cell survival and proliferation. The biochemical pathways involved in this interaction are the same pathways normally used by the immune system to cause B cell proliferation in response to an infection.

The remainder of this chapter is devoted to a brief overview of the relevant biological and immunological features of B lymphocytes and T lymphocytes, both in the context of CLL and, as necessary, in the context of a healthy immune system.

## 1.1 Overview of the Immune System

The immune system is tremendously complicated, and this section is not intended as an exhaustive review of its features and characteristics. Instead, the following will give a brief discussion of the role of B and T lymphocytes in the immune system, how they grow in response to antigen stimulation, and the role of B and T lymphocytes in the immune response. Except where noted, this overview is based on the discussion in Abbas and Lichtman (2005).

### 1.1.1 Antigen Stimulation and Lymphocyte Activation

Any substance (e.g., a surface protein on a virus or a bacterium) that induces an immune response is called an antigen. In response to an antigen, the body manufactures chemicals called antibodies, which can bind to the antigen. The bound antibodies tag the antigen for destruction by cells in the immune system. Both B and T lymphocytes play important roles in this process of antibody production.

The antibodies produced are highly specific, and can only bind to the particular antigen that stimulated antibody production. To achieve this level of specificity, the individual lymphocytes (both B and T) circulating in the body are each capable of reacting to a unique antigen. Lymphocyte stimulation by an antigen causes the lymphocyte to become activated. Normally, there are only a handful of lymphocytes in the body capable of responding to a particular antigen. Once those lymphocytes become activated, however, they undergo chemical changes and rapidly proliferate—a

process called clonal expansion—in order to mount an effective response to the infection.

The specific roles of activated B and T lymphocytes and the interactions between them are discussed below.

### 1.1.2 B Lymphocytes

Activated B cells are responsible for secreting antibodies. Since only the B-cell clones capable of recognizing a particular antigen become active in response to antigen stimulation, the antibodies produced are all capable of binding to the antigen. Normally, however, the antibodies produced by these "naive" lymphocytes do not have a high binding affinity for the antigen, and are not effective enough to combat the infection.

To solve this problem, activated B cells undergo a process called affinity maturation (also called somatic hypermutation). During this process, B cells proliferate rapidly (with a doubling time of roughly 6 to 12 hours) while undergoing extremely high rates of mutation (between $10^3$ and $10^4$ times higher than the background mutation rate in mammals) in the DNA that allows for antigen recognition.

The mutated B cells automatically enter programmed cell death (apoptosis) unless they are rescued by survival signals from both T lymphocytes and other cells in the lymphoid tissue called follicular dendritic cells (FDCs). In order to receive these survival signals, the B lymphocytes must be capable of binding to the relevant antigen. Affinity maturation thus uses selection to produce B-cell mutants with high affinity for that antigen.

### 1.1.3 T Lymphocytes

There are two main types of T lymphocytes: "helper", or CD4+ lymphocytes and "killer", or CD8+ lymphocytes. Killer T cells are cytotoxic cells that are capable of directly killing pathogens and, while immunologically important, are not relevant for the present discussion of B cell activation and CLL.

Helper T cells, on the other hand, play a critical role in the affinity maturation process. Activated B cells express the surface membrane receptor CD40, while helper T cells express the corresponding ligand CD40l on the surface membrane. The CD40:CD40l interaction is one of two necessary signaling pathways to rescue B lymphocytes from apoptosis. In addition to CD40l, T lymphocytes also express antigen receptors. In order to achieve cell to cell contact between B and T cells and thus cause rescue via

CD40:CD40l interaction, a B cell must be capable of taking up an antigen and presenting it on its membrane. This process requires the B cell to have a high affinity for the antigen. Therefore helper T cells are directly responsible for a selective pressure on the mutating B cell population to develop high affinity.

### 1.1.4 Follicular Dendritic Cells and Germinal Centers

The entire process of affinity maturation occurs in the spleen and lymph nodes, which are collectively known as the secondary lymphoid tissue (in contrast with the bone marrow, which is the primary lymphoid tissue). Within the secondary lymphoid tissue, the process takes place in specialized microenvironments called germinal centers. The entire type of immune response under discussion, including B-cell mutation and affinity maturation as well as the behavior of CD4+ helper T cells, is called a germinal-center reaction.

Follicular dendritic cells are structural cells located within the secondary lymphoid tissue, and germinal-center reactions are clustered around the FDCs (Abbas and Lichtman, 2005; Park and Choi, 2005). The mutating B cells and the helper T cells within a germinal center are organized into distinct regions relative to the FDCs, and move between those regions during different stages in the reaction.

Follicular dendritic cells are also responsible for exerting a selective pressure on the mutating B lymphocytes. FDCs take up antigen and present it on the cell surface. The mutated B cells try to bind to this antigen and, if they are successful, receive survival and proliferation signals from the FDC.

## 1.2 Chronic Lymphocytic Leukemia

In chronic lymphocytic leukemia, abnormal B lymphocytes proliferate uncontrollably. These CLL cells share many features with normal B cells. Significantly, CLL co-opts many of the normal mechanisms of lymphocyte survival and growth in germinal-center reactions to prevent cancer-cell death and to promote CLL proliferation.

### 1.2.1 Comparison of B cells and CLL cells

Recent evidence suggests that CLL cells develop from mature B lymphocytes that have been exposed to antigen and have undergone somatic hy-

permutation (Keating et al., 2003). These precursor cells were likely immunocompetent, at one time performing the functions typical of healthy B cells.

Just as significantly, there have been suggestions that CLL cells themselves are still somewhat immunocompetent. CLL cells have been shown to spontaneously undergo many of the chemical and phenotypic changes necessary for somatic hypermutation in vivo, and to do the same in response to external stimuli in vitro (Keating et al., 2003).

### 1.2.2 CLL and T cells

CD4+ helper T cells have been shown to decrease the rate of apoptosis of CLL cells in vitro (Caligaris-Cappio and Dalla-Favera, 2005). The same experiment showed soluble CD40l (sCD40l) to have a similar effect, which suggests that T-cell rescue of CLL cells is mediated by the same CD40:CD40l interaction that rescues normal B cells.

These in vitro experiments with T lymphocytes and sCD40l were unable to keep CLL cells alive indefinitely. The interpretation of this finding in the literature is unclear, but it could suggest either that the in vitro environment does not approximate the cancer's in vivo microenvironment—for example the in vivo situation could include a continual resupply of CD40l from new T cells—or that other factors are ultimately more important for CLL survival in vitro.

### 1.2.3 Chronic Lymphocytic Leukemia (CLL) and Follicular Dendritic Cells (FDCs)

Although it will not be used for our present work, FDCs have also been shown to promote CLL growth and survival in vitro, and over a longer timescale than do T cells (Caligaris-Cappio and Dalla-Favera, 2005). The mechanism behind FDC dependent rescue is not well understood.

Samples of lymphoid tissue from some cases of CLL show the existence of cancer "proliferation centers", which may be roughly analogous to normal germinal centers, although this feature is not present in all cases of the disease (Keating et al., 2003).

### 1.2.4 Chemotaxis

CLL cells have the ability to reshape their microenvironment into one more conducive to cancer growth by exploiting the process of chemotaxis. Chemo-

taxis is a method of cell movement by which cells move in response to gradients in the concentration of a particular chemical, called a chemokine. For example, a population of chemotactically sensitive cells may move from a region of low chemokine concentration to a region of high concentration. In a normal immune system, chemotaxis is used extensively to direct specific immune cells to different locations within the body or to regions within a particular tissue (Abbas and Lichtman, 2005).

CLL cells are capable of secreting at least two chemokines (and potentially many others). In response to CD40l stimulation, CLL cells produce the chemokine CCL22, which attracts CD4+ T cells (Ghia et al., 2002; Caligaris-Cappio, 2003). Since CD4+ T cells express CD40l, this suggests a positive feedback loop whereby T lymphocytes incite CCL22 production in CLL cells, which in turn attracts more T lymphocytes.

In addition, CLL cells secrete the chemokine interleukin-8 (IL-8), which actually attracts other CLL cells. IL-8 only allows CLL cells to move along strands of hyaluronan (HA), a molecule which is present in certain regions within the secondary lymphoid tissue (Till et al., 1999). So not only does CLL attract other cells required for its survival, the cancer cells themselves also have the potential to aggregate within the lymphoid tissue.

### 1.2.5 Conclusion

Altogether, these results paint a picture of CLL as disease that is dependent on many of the same chemical pathways and processes as normal B lymphocyte proliferation and survival. Moreover, CLL cells are able to actively reshape their local environment via the secretion of chemokines into a microenvironment that encourages cancer growth. Such positive feedback mechanisms provide a compelling picture for how CLL growth is dependent on—and benefits from—other cells such as CD4+ T cells and FDCs.

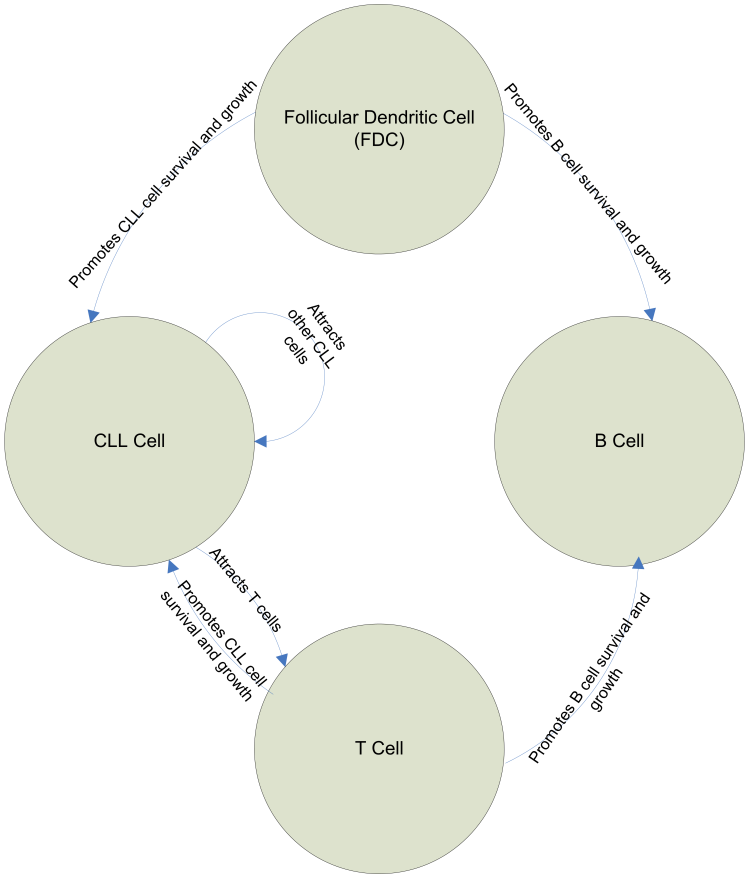


Figure 1.1: Schematic diagram of interactions between CLL cells, B cells, T cells, and FDCs. See Chapter 1 for details.

# Chapter 2

# Prior Mathematical Work

Very few mathematical models of CLL have been developed to date, and no models have been developed that incorporate spatial phenomena such as chemotaxis. There have, however, been a small number of nonspatial models. Substantial work has also been performed on modeling chemotaxis in general. This chapter will briefly review earlier research done in both of these areas.

## 2.1 ODE Models of CLL

Models of CLL to date have used models employing systems of ordinary differential equations (ODEs) to study the dynamics of leukemia growth (see Martinis et al. (2005); Vitale et al. (2003); Messmer et al. (2005); Kuznetsov et al. (1994)). Much of this work has focused on modeling the interaction between the immune system and CLL by considering the total populations of CLL cells and immune cells in a patient's body. A Volterra-type population model was used to simulate the destruction of CLL cells by "predator" T lymphocytes (Martinis et al., 2005; Vitale et al., 2003). A more complicated model involving reaction kinetics based on an intermediate population of CLL-immune cell complexes was developed to study the destruction of CLL cells by cytotoxic natural killer cells (Kuznetsov et al., 1994).

These ODE models have produced useful results using techniques from dynamical systems to identify regions of the parameter space where the cancer grows more quickly or less quickly. The analysis in Kuznetsov et al. (1994) even provided an explanation for an observed phenomenon in which the cancer appears to be under control for a long time prior to suddenly

growing rapidly into a large tumor.

In contrast, the model in Messmer et al. (2005) focused only on CLL cells, but used a compartmental model to separate the populations of CLL cells in the peripheral blood from those cells in the lymphoid tissue. This model was used in conjunction with a clinical experiment that tracked the production of new CLL cells by giving patients doses of heavy water, which tagged CLL cells produced during heavy-water dosing. The measurement of tagged and untagged CLL cells over time was used to conclude that CLL cells typically have a rapid growth rate coupled with a nearly as fast death rate. The discovery of these high rates was contrary to the prevailing dogma of CLL as a disease characterized by slow but steady growth of cancer cells (Messmer et al., 2005).

To date these are the only models of CLL of which we are aware, and we know of no other published or forthcoming mathematical models of CLL that study the effects of microenvironmental or spatial factors on cancer growth (with the exception of the compartment model in Messmer et al. (2005)). Furthermore, all immunological models have focused on the role of the immune system in limiting cancer growth, and not on the necessary role the immune system plays in promoting CLL growth.

## 2.2 Models of Chemotaxis

There has been extensive work on partial differential equation models of chemotaxis. The canonical model, called the Keller–Segel model (see Keller and Segel, 1971), tracks the movement of one cell population in response to a chemokine distribution as a system of advection-diffusion-reaction equations of the form

$$\begin{aligned} \frac{\partial n}{\partial t} &= \nabla \cdot (D_n(c)\nabla n - \chi(c) n \nabla c) \\ \frac{\partial c}{\partial t} &= D_c \Delta c - n\delta(c), \end{aligned} \tag{2.1}$$

where $n(\underline{x}, t)$ is the density of cells, $c(\underline{x}, t)$ is the concentration of chemokine, and $\underline{x} = (x, y)$ is the position within a two-dimensional domain.

Cellular movement—whether directed or random—is considered to be influenced by the chemokine. Cellular diffusion is dependent on the chemokine concentration through the $D_n(c)$ coefficient, whereas advection is dependent on the concentration of chemokine through the $\chi(c)$ coefficient and on the chemokine gradient $\nabla c$. The chemokine moves by linear diffu-

sion with diffusion constant $D_c$, and is degraded via uptake by cells with rate $\delta(c)$.

The functional forms of $D_n(c)$, $\chi(c)$, and $\delta(c)$ are obviously critical to determining the behavior and biological relevance of Equation 2.1. Several common and mathematically simple choices for these functional forms are discussed in Sherratt (1994).

In Sherratt et al. (1993), a new model for chemotaxis is proposed that realistically models the chemokine-receptor dynamics on the cell surface, which was shown to have excellent agreement with experimental data on chemotaxis. This model involves a larger and more complicated system of partial differential equations than the Keller–Segel model. In Sherratt (1994), however, minor simplifications to the previous model are shown to reduce it to a system of Keller–Segel form that also agrees well with experiment.

These simplifications yield the following functional forms:

$$\begin{aligned} D_n(c) =& [D_0(k_d+k_i)^2 + \{2D_0(1-\beta\Gamma) + D_1\Gamma\}\,(k_d+k_i)k_a c + \{D_0(1-\beta\Gamma)^2 \\ &+ D_1\Gamma(1-\beta\Gamma) - D_2\Gamma^2\}k_a^2c^2]\,/\,[k_d+k_i+(1-\beta\Gamma)k_a c]^2 \end{aligned} \tag{2.2a}$$

$$\chi(c) = \frac{\chi_0 k_a \Gamma(k_d+k_i)}{[k_d+k_i+(1-\beta\Gamma)k_a c]^2} \tag{2.2b}$$

$$\delta(c) = \frac{\Gamma k_i k_a c}{k_d+k_i+(1-\beta\Gamma)k_a c}. \tag{2.2c}$$

The constants in Equation 2.2 are all experimentally measurable quantities. The $k_d$, $k_i$, and $k_a$ terms govern the chemical reaction between cell surface receptors and chemokines; $\beta$ and $\Gamma$ are related to the number of receptors on the cell surface; and $D_0$, $D_1$, $D_2$, and $\chi_0$ are coefficients for the various terms in the expressions for diffusion and chemotaxis (for details, see Sherratt et al., 1993). While these equations are algebraically formidable, they are not computationally challenging, and yield a biologically and chemically realistic picture of chemotaxis (Sherratt et al., 1993; Sherratt, 1994).

We will apply these functional forms for the Keller-Segel equations to our model of chemotaxis for CLL and T cells in Chapter 3.

# Chapter 3

# Spatial Model of CLL Dynamics

In this chapter, we develop a mathematical model of CLL that focuses on the interactions between CLL cells and CD4+ CD40L+ T cells within the secondary lymphoid tissue. In particular, we model the ability of T cells to promote CLL cell survival and proliferation through direct cell-to-cell contacts. Additionally, we model changes in the spatial distributions of both CLL and T cells due to both random cell movement and directed cell movement in response to chemotactic signals. To incorporate the latter effect, we also model the secretion, diffusion, and uptake of the chemokines IL-8 and CCL22 by CLL cells.

Section 3.1 will provide a brief overview of the model, including model equations and intuitive explanations of the various terms in those equations. In Section 3.2 we will move into a more detailed explanation and justification of our modeling choices. In Section 3.3 we will discuss the geometry on which the model is solved and the relevant boundary conditions for this geometry.

## 3.1 Model Overview

We chose to model the populations of CLL cells and T cells and the concentrations of IL-8 and CCL22 as a system of four partial differential equations.

Letting our state variables be the CLL cell density $b(\underline{x}, t)$ and T-cell population density $h(\underline{x}, t)$[1], both in cells per liter (cells/L), and the concentra-

[1]The letter $h$ was chosen in reference to the phrase "helper T cell", another common

tions of IL-8 $i(\underline{x}, t)$ and CCL22 $c(\underline{x}, t)$, both in mol/L, we constructed the following general system:

$$\begin{aligned}
\frac{\partial b}{\partial t}(\underline{x}, t) &= \nabla \cdot [D_b(i)\nabla b - \chi_b(i) b \nabla i] + f_b(b, h) - g_b(b, h) \\
\frac{\partial h}{\partial t}(\underline{x}, t) &= \nabla \cdot [D_h(c)\nabla h - \chi_h(c) h \nabla c] \\
\frac{\partial c}{\partial t}(\underline{x}, t) &= D_c \Delta c + f_c(b, h, c) - g_c(h, c) \\
\frac{\partial i}{\partial t}(\underline{x}, t) &= D_i \Delta i + f_i(b, i) - g_i(b, i).
\end{aligned} \tag{3.1}$$

Each of the terms in Equation 3.1 will receive a detailed treatment in Section 3.2, but for now they can be divided into the three broad categories of diffusion, chemotaxis, and reaction terms.

The diffusion terms are of the form

$$\nabla \cdot (D_u \nabla u), \tag{3.2}$$

where $D_u$ is the (possibly spatially varying) diffusion coefficient and $u$ is an arbitrary dependent variable (so $u$ is a stand-in for $b$, $h$, $c$, or $i$).

In the case of chemokine diffusion (i.e., for IL-8 and CCL22), the diffusion coefficient $D_u$ is taken to be constant so that Equation 3.2 reduces to the linear diffusion equation

$$D_u \Delta u,$$

whereas for cellular diffusion the coefficient is a function of chemokine concentration (see Sections 1.2.4, 2.2, and 3.2).

The chemotaxis terms, which only appear in the state equations for the two cell populations, are of the form

$$-\nabla \cdot (\chi_u(k) u \nabla k),$$

where $k$ is the relevant chemokine concentration. The coefficient $\chi_u$ is called the chemotactic coefficient for $u$, and is taken to be dependent on $k$ (again, see Sections 1.2.4, 2.2, and 3.2).

The reaction terms are those terms of the form

$$f_u - g_u.$$

---

name for CD4+ T cells.

Throughout this thesis we adopt the convention that $f_u \geq 0$ and $g_u \geq 0$, so that $f_u$ and $g_u$ correspond with the rates at which $u$ is being produced and eliminated, respectively.

Note that the physical interpretations of $f_u$ and $g_u$ may vary. For example, in the case of one of our chemokines they may be the rates of secretion and uptake, respectively, whereas for a cell population they will represent rates of cell division and cell death.

Together, the diffusion, chemotaxis, and reaction terms give an intuitive picture of how the dependent variables $b$, $h$, $c$, and $i$ can change and interact. With this picture in mind, we can turn to a more detailed study of each of these expressions.

## 3.2 Model Explanation and Justification

### 3.2.1 Cell Movement

The chemotactic and diffusive movement of CLL cells and T cells follows the general form of the Keller–Segel model discussed in Section 2.2 and Sherratt (1994). Recall that in this model, a cell population $n$ and a chemokine concentration $c$ are governed by the partial differential equations

$$\frac{\partial n}{\partial t} = \nabla \cdot (D_n(c)\nabla n - \chi(c) n \nabla c)$$
$$\frac{\partial c}{\partial t} = D_c \Delta c - n\delta(c).$$

While the Keller–Segel model is not specific to a particular type of eukaryotic cell, the particular functional forms for $D_n(c)$, $\chi(c)$, and $\delta(c)$ are. The analysis in Sherratt (1994) produces expressions for these three terms in the case of neutrophils being attracted by a peptide concentration gradient.

For our model, we make the assumption that both CLL and T-cell populations can also be modeled with these particular functional forms. We justify these assumptions in two ways. First, neutrophil–peptide interactions are one of the best-studied chemotactic systems. To our knowledge, CLL cell and T-cell chemotaxis has not been well studied. Given that neutrophils, CLL cells, and T cells are all motile immune cells, it seems reasonable to approximate the movement of the latter two with the former until better data becomes available. Second, the assumptions in Sherratt (1994) used to produce the given functional forms are also reasonable to assume in both CLL and T-cell chemotaxis. These assumptions are that the size of an individual cell is small compared to the size of the whole domain, and that

the chemical interactions between chemokines and their receptors occur on a much faster timescale than does cell movement. So while our parameter values may be different than in a neutrophil-peptide system, the form of the model itself should still be valid.

### 3.2.2 CLL Cell T Cell reactions

In Section 1.2.2, we discussed how CD40:CD40l interactions between CLL cells and T cells promote CLL cell survival and proliferation. Because $f_b$ represents CLL cell growth whereas $g_b$ represents cell death, in the absence of T cells $g_b$ should be large compared to $f_b$ and in the presence of T cells the reverse should be true.

To model this relationship between CLL growth and death and the presence of T cells, we chose to express cell growth as

$$f_b(b,h) = \beta_b \frac{bh}{s+h}$$

and

$$g_b(b,h) = \delta_b b \left(1 - \frac{h}{s+h}\right),$$

where $\beta_b$ and $\delta_b$ are birth-rate and death-rate constants, and $s$ is a constant whose role is explained below.

These functional forms are clearly phenomenological, and should not be expected to give any insight into the mechanism of CD40:CD40l interactions. However, note that as $h \to 0$, $f_b \to 0$ and $g_b \to \delta_b b$, and that as $h \to \infty$, $f_b \to \beta_b b$ and $g_b \to 0$. This means that these terms have the desired qualitative behavior.

The constant $s$ is the concentration of T cells such that the ratio

$$\frac{h}{s+h}$$

equals $\frac{1}{2}$ when $h = s$. This "halfway to maximum" value is not necessarily physically relevant, and should just be interpreted as an additional parameter of the model.

### 3.2.3 Chemokine Secretion and Uptake

The reaction terms $f_c$, $g_c$, $f_i$, and $g_i$ governing the secretion of CCL22 and IL-8 by CLL cells and the uptake of those chemokines by T cells and CLL cells are derived in two different ways.

The uptake functions $g_c$ and $g_i$ are found as part of the analysis of receptor dynamics in Sherratt (1994), and we use those forms in our model (see Section 2.2).

Recalling from Section 1.2.4 that CLL cells secrete IL-8, we choose to model IL-8 secretion as a mass action reaction by

$$f_i(b) = \beta_i b.$$

Similarly, because CLL cells secrete CCL22 in response to T-cell stimulation we model CCL22 secretion as

$$f_c(b,h) = \beta_c bh.$$

These mass-action terms are, like the CLL-reaction terms, highly phenomenological. We choose them mainly for mathematical convenience in the absence of experimental data that would suggest a better functional form.

## 3.3 Model Geometry and Boundary Conditions

So far, we have avoided specifying either a domain for the system of PDEs in Equation 3.1 or boundary conditions on the edges of a domain. Since the spatial dynamics we have been describing occur within the secondary lymphoid tissue (the spleen and the lymph nodes), we chose to to solve our PDEs on a $3 \cdot 10^{-3}$ m by $1 \cdot 10^{-3}$ m rectangular domain, roughly the size of a small lymph node. The numerical method used to solve our equations (see Chapter 4) allowed us to easily implement other domains, and so we also studied a circular domain. We chose the rectangular shape for the ease with which we could implement boundary conditions.

We chose to use a no-flux boundary condition. Thus for the CLL cell population we have

$$\underline{n} \cdot (-D_b(i)\nabla b + \chi_b(i) b \nabla i) = 0, \tag{3.3}$$

where $\underline{n}$ is the outward unit normal to the boundary and the term in parentheses is the flux of CLL cells. The equation for the T-cell population is similar. Note that in Equation 3.3, the flux is the sum of a diffusive term $-D_b(i)\nabla b$ and a chemotactic term $\chi_b(i) b \nabla i$, and that these terms have opposite signs from one another. This sign difference is easily explained. When cells diffuse they move from regions of high density into regions of low density, which means they move in the direction of $-\nabla b$. When cells

move chemotactically, however, they move from regions of low chemokine concentration to regions of high chemokine concentration, meaning they move in the direction of $\nabla i$. Since $D_b(i)$, $\chi_b(i)$, and $b$ are all non-negative, the terms in our flux expression have the correct sign.

The no-flux boundary conditions for the chemokine concentrations are similar to those for the cell populations, but here the only contribution to the flux is from diffusion. This gives

$$\underline{n} \cdot (-D_c \nabla c) = 0,$$

and similarly for $i$.

We justify the no-flux boundary condition by assuming that neither cells nor chemicals can leave the lymph node under consideration. This assumption is obviously not entirely accurate, as cells do enter and exit lymphoid tissue at specific points. Expanding the model to incorporate this feature is certainly an area for future work (see Chapter 6).

# Chapter 4

# Numerics

The partial differential equation model developed in Chapter 3 was solved numerically using version 3.5a of the COMSOL Multiphysics software package (see `http://www.comsol.com/`), a commercial finite-element method solver. No additional modules beyond the core software were required for our problem.

## 4.1 COMSOL Model Setup

The system of PDEs in Equation 3.1 involves four state variables, so we used the multiphysics feature of COMSOL to develop a model file with an application mode for each of CLL cells, T cells, CCL22, and IL-8. For CLL and T cells, we used the Convection and Diffusion application mode, and for CCL22 and IL-8, we used the Diffusion application mode. In the case of the Convection and Diffusion mode, multiple modifications to COMSOL's default settings were necessary to obtain satisfactory numerical results, which we detail below.

During implementation of the model, preliminary testing of the chemotaxis and diffusion terms showed that COMSOL does not automatically conserve the total cell population, because the advection diffusion equation in COMSOL is given in a nonconservative form by default, as

$$\frac{\partial n}{\partial t} = \nabla \cdot (D \nabla n) - u \cdot \nabla n,$$

where $u$ is the local speed of advection. This form results from "multiplying through" the divergence of the advection term in the expression for the flux of $n$. To solve this problem, it was necessary to use the application mode

properties dialog box to change the Equation type to conservative, which required COMSOL to solve an equation of the form

$$\frac{\partial n}{\partial t} = \nabla \cdot (D\nabla n - un) .$$

Subsequent numerical experiments confirmed that this change conserved the total quantity of cells present.

During further testing, we also discovered that COMSOL's numerical solver produces oscillatory solutions. We were unable to find a method within the software package for changing to a nonoscillatory numerical scheme. To minimize the extent of these oscillations, we chose to change the element COMSOL used in its finite-element method from a quartic to a quintic Lagrange polynomial. While this change did not eliminate the oscillations, it did make them much smaller in magnitude.

Finally, we also found it necessary to introduce artificial diffusion terms into the CLL-cell and T-cell application modes in order to prevent the solution from becoming unstable. COMSOL presents a number of artificial diffusion options, and on the recommendation of COMSOL's documentation we chose to use Petrov–Galerkin compensated streamline diffusion with a tuning parameter of $\delta_{sd} = 0.25$.

Unfortunately, we could not find detailed documentation of exactly how this type of artificial diffusion works, although the help file within the COMSOL application suggests that it introduces diffusion in locations where advection dominates over the actual diffusion term, while leaving regions where diffusion dominates unaltered. This change allowed us to produce stable solutions.

# Chapter 5

# Results

Our simulations produced two surprising results that may be both biologically and clinically relevant, as well as one numerical issue that warrants careful investigation. We present our results here and discuss their potential implications in Chapter 6.

## 5.1 CLL Cells Fail to Reshape Their Microenvironment

First, recall that our purpose in developing a PDE model was to investigate spatial effects on cancer growth. In Chapter 1 we mentioned that CLL cells secrete chemokines that may be important in reshaping the cancer microenvironment. In our model, however, we were unable to find biologically realistic initial conditions for which the movement of either CLL or T cells proved important for disease progression. In particular, we found that when the initial density of T cells was too low for net CLL growth, it remained too low rather than gathering together to cause a region of net growth. This failure to reshape the microenvironment appeared to be at least partially due to the chemokines diffusing much more quickly than the cell populations could move, which meant that chemokine concentration gradients—and, therefore, chemotactic effects—were small.

## 5.2 External Chemokine Gradients Appear to Influence Disease Progression

In light of this first result, we chose to see whether there were other ways in which chemotaxis might be important. In particular, we investigated

whether an externally maintained chemokine gradient might cause changes to disease progression. To maintain such an external gradient, we reformulated the boundary conditions on the edges of our $3 \cdot 10^{-3}$ m by $1 \cdot 10^{-3}$ m rectangle for both chemokines to be of the form

$$\begin{cases} c(x,0,t) = 0, & 0 < x < 3 \cdot 10^{-3}, \\ c(0,y,t) = 0, & 0 < y < 1 \cdot 10^{-3}, \\ c(x,1 \cdot 10^{-3},t) = c_0 \frac{x}{3 \cdot 10^{-3}} & 0 < x < 3 \cdot 10^{-3}, \\ c(3 \cdot 10^{-3},y,t) = c_0 \frac{y}{1 \cdot 10^{-3}}, & 0 < y < 1 \cdot 10^{-3}, \end{cases}$$

and similarly for $i(x,y,t)$. Here, the constants $c_0$ and $i_0$ were both set to $1 \cdot 10^{-8}$ mol $L^{-1}$ (see Appendix A for a discussion of parameter values).

With these Dirichlet boundary conditions, we used COMSOL to find the steady-state solutions to the diffusion equations for $c$ and $i$ in the absence of reactions, and used these solutions as the initial conditions for $c$ and $i$ in our model (see Figure 5.1). Because chemokine diffusion was faster than the other processes in our model, the chemokine concentrations would stay at approximately steady state throughout the simulation.

For our cell populations, we chose to have initially constant densities of both cell types, with 25,000 cells per liter. In the absence of cell movement, the reaction terms in our model would have caused a net cancer decline from these starting densities, since the T cell density was too low to cause growth.

We simulated ten days of activity, and found that the steady chemokine gradients were able to attract a sufficiently high number of CLL and T cells during that time to reverse the disease course from net death to net growth (see Figures 5.2 and 5.3). At first the overall CLL cell population declined, but as more cells aggregated together in the top left corner of the domain, the cancer began to grow.

## 5.3 Numerical Artifacts

We encountered one problem with COMSOL's numerical solution that we were unable to resolve. At early times in the above simulation, we observed small regions within the domain in which the CLL cell density had either a positive or negative peak (see Figure 5.4(a)). These peaks are certainly not physical—a density cannot be negative—and there is no reason to expect such behavior from the PDEs themselves. Thus we conclude that these peaks are numerical artifacts from COMSOL's numerical scheme. By 20

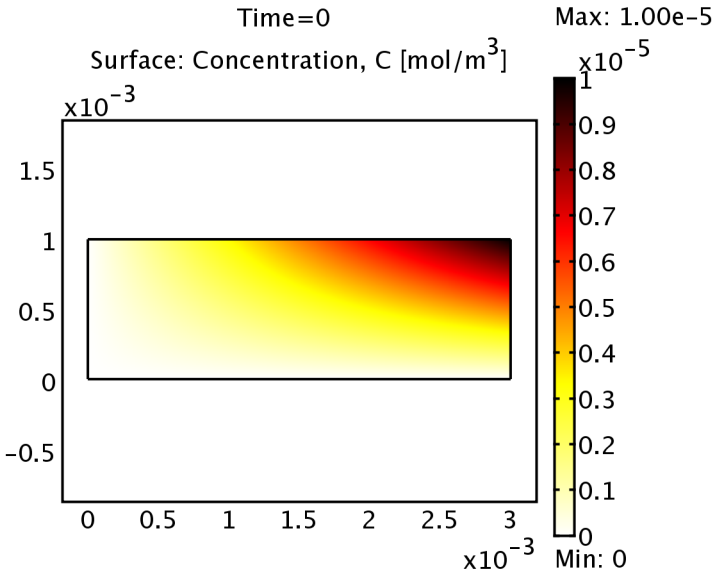


Figure 5.1: Steady-state concentration of CCL22 chemokine with the Dirichlet boundary conditions of zero on the lower and left walls and linearly varying between 0 and a constant concentration on the upper and right walls. Here $C = C(\underline{x})$ represents the concentration of CCL22.

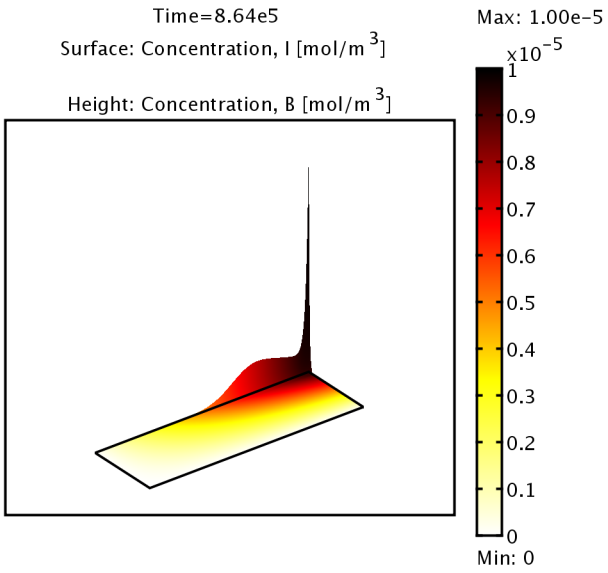


Figure 5.2: CLL cell density (surface data) and IL-8 concentration (color data) after 10 days. CLL cells were originally at a constant density and IL-8 was at steady-state concentration. Note that the CLL cells have migrated up the IL-8 concentration gradient toward the far corner. The maximum CLL cell density in the far corner of the domain is $8.099 \cdot 10^{-14}$ mol m$^{-3}$, which is compared with a uniform initial density of $4.151 \cdot 10^{-17}$ mol m$^{-3}$. Here $I = I(\underline{x})$ and $B = B(\underline{x})$ represent the concentration of IL-8 and the density of CLL cells, respectively.

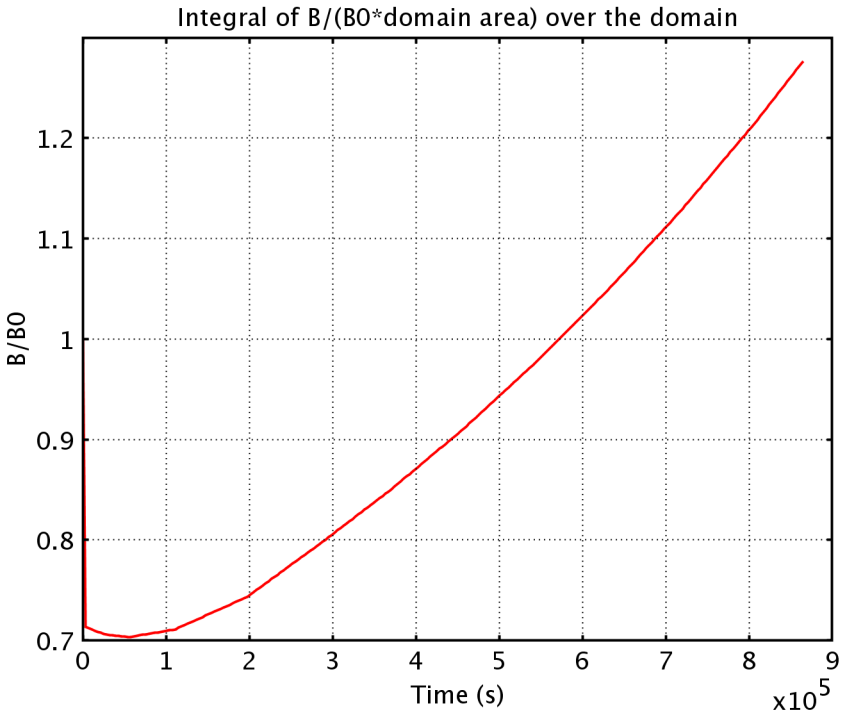


Figure 5.3: Normalized integral of CLL cell density over the rectangular domain. Time ranges from 0 to 10 days, and is given in seconds. Note that the integral initially decreases, but as the CLL and T cells cluster, the T-cell density becomes sufficiently high to encourage CLL cell growth, and the integral begins to increase. Here $B = B(\underline{x})$ represents the density of CLL cells and $B_0$ is the initial density of CLL cells at the start of the simulation.

hours into the 10-day simulation, these artifacts are largely overwhelmed by the model's expected behavior (Figure 5.4(b)), so it is unclear whether they have a meaningful influence on the long-term solution.

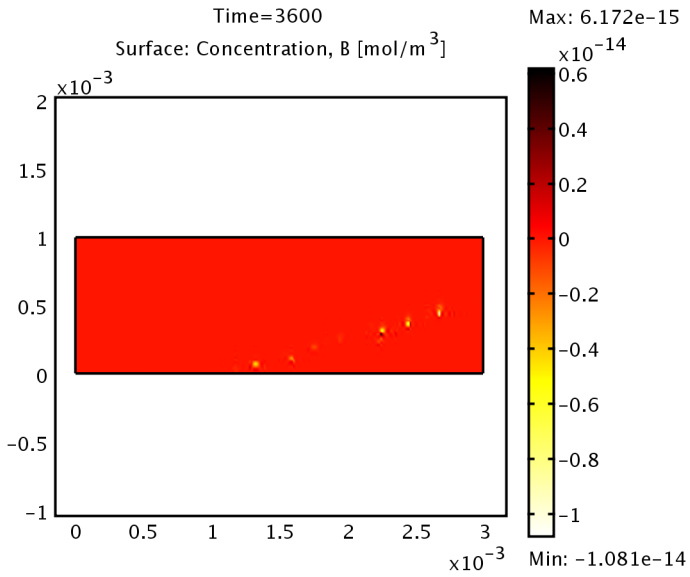


(a) One hour into simulation.

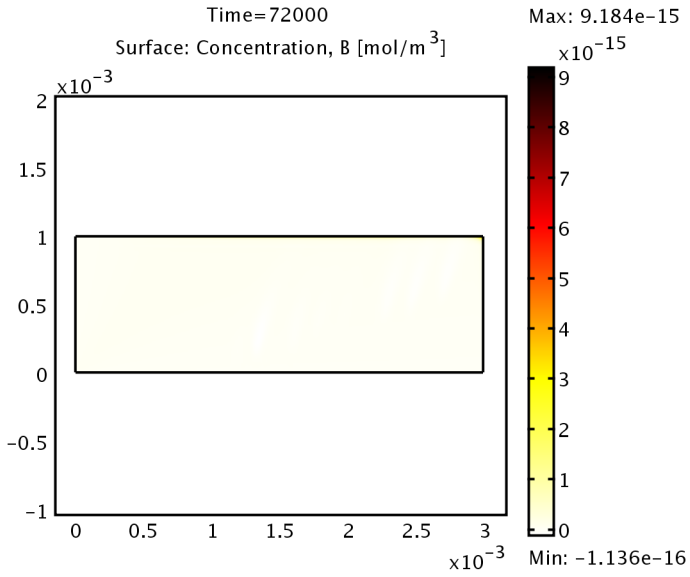


(b) Twenty hours into simulation.

Figure 5.4: Numerical artifacts produced early in simulation of CLL movement with respect to steady chemokine gradient. Note that the simulation runs for a total of 10 days, and by 20 hours the artifacts are largely overwhelmed by the expected behavior of the system. Here $B = B(\underline{x})$ represents the density of CLL cells.

# Chapter 6

# Discussion

The results generated by our model have interesting implications for the biology of chronic lymphocytic leukemia. CLL cells in the model were unable to effectively reshape their microenvironment into one that would foster cancer growth. Of course this does not necessarily imply that the same is true in vivo, but it does mean that more mathematical and experimental investigation is required to nail down this issue. In particular, we should note that neither in vitro nor in silico efforts have been able to show how CLL cells remain viable in vivo. Moreover, while much of the work referenced in Chapter 1 showed that CLL cells are capable of secreting the chemokines necessary for such a remodeling of the microenvironment (Ghia et al., 2002; Caligaris-Cappio, 2003; Till et al., 1999), none of these experiments demonstrated that such a phenomenon actually takes place either in vivo or in vitro.

While we are certainly not qualified to make claims about the feasibility of any particular biological experiment, we expect that a reasonable first step toward resolving this issue would be to perform in vitro chemotactic assays involving CLL cells and T cells.

Computationally, the fact that the model was unable to produce one of our expected results means that the equations themselves should be reexamined. In particular, note that the reaction terms derived in Chapter 3 are of a phenomenological origin—they were designed to reflect the observation that at low T-cell densities CLL cells die, while at high T-cell densities they survive and proliferate. A more mechanistic approach that realistically modeled the biochemical interactions between our two cell populations, as well as the secretion of chemokines, might yield different results. At the very least, if a more mechanistic model reproduced the result found

here, we would be more confident in the conclusion that CLL cells cannot reshape their environment through the CCL22 and IL-8 pathways than we are at present.

Our model's second result, that an externally maintained chemokine gradient can alter the cancer's course, is at least as biologically intriguing as the above discussion. We do not know what could create such a gradient in vivo, and will not even attempt to name any potential candidates. Perhaps it is going too far to say that the existence of such an external gradient is a prediction of our model, because it could also be the case that chemotactic effects are important and that there are other nonspatial factors we have not considered, but the experimental discovery of such a gradient would be a form of validation for this model. A more exhaustive study of the cell types residing in lymphoid tissue should be performed to see whether any of them are capable of producing and maintaining a chemokine gradient of this type.

The numerical artifacts discussed in Section 5.3 are certainly disturbing, and every effort should be made to eliminate them in order to verify that our numerical results correctly capture the behavior of our PDEs. COMSOL was used extensively on this project for the ease and speed with which solutions to nonlinear systems of PDEs can be computed. It is likely, however, that the best way to eliminate these numerical difficulties is to switch to a scheme designed specifically for strongly hyperbolic problems such as ours. Such an approach would certainly allow much finer control over the computational details than COMSOL seems to permit. One possibility is to implement a high-order, nonoscillatory, finite-volume method specifically designed for hyperbolic problems (see LeVeque, 2002). Such an undertaking would be more time consuming than using a ready-made package such as COMSOL, but would likely produce better results.

It is true that to be fully confident in our model's results we need to eliminate these numerical problems. At the same time, recall that these problems were transient, and had become small compared to the rest of the solution relatively early in the simulation. The solution's long-term behavior agreed more closely with our intuition about the types of behavior the PDEs should produce. So it is not certain that resolving these issues would change the biological statements of our model.

# Chapter 7

# Conclusion

We have described a simple system of four partial differential equations that models the interplay between chronic lymphocytic leukemia and CD4+ T cells. Testing this model has had interesting outcomes from mathematical and biological standpoints. Mathematically, we have encountered substantial numerical difficulties in solving our PDEs, and future computational work to resolve these problems should be conducted. In addition, we discussed in Chapter 6 that refining the model to include more biochemically realistic reactions between CLL and T cells may yield interesting results and will certainly increase our confidence in the model's biological relevance.

Our major biological result was that—contrary to what might be concluded from the experimental work discussed in Section 1.2—CLL cells may not have the ability to actively reshape their own microenvironment, but rather might be at the mercy of some other force responsible for the spatial organization of lymphoid tissue. The hypotheses that CLL cells are unable to effectively reshape their microenvironment and that other cellular or chemical players are necessary for cancer growth are both rich and potentially clinically relevant areas for future experimental work.

# Appendix A

# Parameter Values

Parameter values are summarized in Table A.1, and are explained below.

## A.1 Derivation of Parameter Values

The parameters involved in chemotaxis were taken from earlier work on the chemotaxis of neutrophils (Sherratt et al., 1993; Sherratt, 1994), which we discussed in detail in Section 2.2. Recall that we argued that because of the absence of chemotactic assays for CLL cells (or even healthy B cells), and for T cells, we made the assumption that our cell populations could be approximated with the parameter values for a neutrophil population.

The initial population densities $b_0$ and $h_0$ for CLL cells and T cells were taken from experimental work on these cell types (Caligaris-Cappio, 2003; Caligaris-Cappio and Dalla-Favera, 2005). The initial concentration $c_0$ of CCL22 was taken as an order of magnitude estimate from Ghia et al. (2002). In the absence of data, the same concentration was assumed as a reasonable initial concentration for $i_0$.

The birth and death rates, $\beta_b$ and $\delta_b$, for CLL cells were derived from the experiments in Caligaris-Cappio and Dalla-Favera (2005) as follows. In those experiments, populations of CLL cells were exposed to T cells as well as soluble CD40l. We assumed that in those cultures, chemotaxis was negligible and that all populations and chemicals were initially well-mixed. This assumption allowed us to consider the reaction terms from our PDE model as a simple ODE of the form

$$\frac{db}{dt} = \beta_b \frac{bh}{s+h} - \delta_b b \left(1 - \frac{h}{s+h}\right)$$

| Parameter | Value | Description |
|---|---|---|
| $D_{b0}$ | $1.3 \cdot 10^{-10}$ cm$^2$ s$^{-1}$ | Parameters $D_{b0}$ through $\chi_{h0}$ are parameters involved in chemotaxis. See Section 2.2. |
| $D_{b1}$ | $4.8 \cdot 10^{9}$ cm$^2$ s$^{-1}$ mol$^{-1}$ | |
| $D_{b2}$ | $3 \cdot 10^{28}$ cm$^2$ s$^{-1}$ mol$^{-2}$ | |
| $\Gamma_b$ | $4.98 \cdot 10^{-21}$ mol | |
| $\mu_b$ | $1.95 \cdot 10^{20}$ mol$^{-1}$ | |
| $k_{bd}$ | 0.35 min$^{-1}$ | |
| $k_{bi}$ | 0.24 min$^{-1}$ | |
| $k_{ba}$ | $1 \cdot 10^{9}$ L mol$^{-1}$ min$^{-1}$ | |
| $\chi_{b0}$ | $2 \cdot 10^{12}$ cm$^2$ s$^{-1}$ mol$^{-1}$ | |
| $D_{h0}$ | $1.3 \cdot 10^{-10}$ cm$^2$ s$^{-1}$ | |
| $D_{h1}$ | $4.8 \cdot 10^{9}$ cm$^2$ s$^{-1}$ mol$^{-1}$ | |
| $D_{h2}$ | $3 \cdot 10^{28}$ cm$^2$ s$^{-1}$ mol$^{-2}$ | |
| $\Gamma_h$ | $4.98 \cdot 10^{-21}$ mol | |
| $\mu_h$ | $1.95 \cdot 10^{20}$ mol$^{-1}$ | |
| $k_{hd}$ | 0.35 min$^{-1}$ | |
| $k_{hi}$ | 0.24 min$^{-1}$ | |
| $k_{ha}$ | $1 \cdot 10^{9}$ L mol$^{-1}$ min$^{-1}$ | |
| $\chi_{h0}$ | $2 \cdot 10^{12}$ cm$^2$ s$^{-1}$ mol$^{-1}$ | |
| $b_0$ | 25000 cells L$^{-1}$ | Initial CLL cell density |
| $h_0$ | 25000 cells L$^{-1}$ | Initial T cell density |
| $c_0$ | $1 \cdot 10^{-8}$ mol L$^{-1}$ | Initial CCL22 concentration |
| $i_0$ | $1 \cdot 10^{-8}$ mol L$^{-1}$ | Initial IL-8 concentration |
| $\beta_b$ | $1 \cdot 10^{-6}$ cells s$^{-1}$ | CLL cell growth rate coefficient |
| $\delta_b$ | $1 \cdot 10^{-6}$ cells s$^{-1}$ | CLL cell death rate coefficient |
| $s$ | 100000 cells L$^{-1}$ | Constant in CLL reaction terms |

Table A.1: Parameter values for the model derived in Chapter 3. Justifications and derivations are given in Appendix A, as appropriate.

for a known density $h$ of T cells.

This equation is easily solvable in terms of $s, \beta_b, \delta_b$, and a constant of integration $A$ giving

$$b(t) = Ae^{rt},$$

where $r = \beta_b \frac{h}{s+h} - \delta_b \left(1 - \frac{h}{s+h}\right)$.

We fit the temporal data for CLL cells from Caligaris-Cappio and Dalla-Favera (2005) to this form using a least-squares method. For the sake of finding reasonable parameter values, we made the assumption that $\beta_b$ and $\delta_b$ were equal, and under this assumption we made a guess of the value of $s$ by comparing the values of $\beta_b$ and $\delta_b$ for different values of $s$ with the birth rates and death rates given in Messmer et al. (2005). Note that we chose this course rather than simply using the rates given in Messmer et al. (2005) because those rates were overall birth and death of CLL in human patients, which we took to be appropriate as a check on the plausibility of our calculation, but to be skewed by the fact that it already includes the interaction between CLL cells, T cells, and numerous other cells in a way that obscures what the T cell independent rates would be.

# Bibliography


Abbas, Abul K., and Andrew H. Lichtman. 2005. *Cellular and Molecular Immunology*. Philadelphia, PA: Saunders, 5th ed. 1, 1.1, 1.1.4, 1.2.4

Caligaris-Cappio, F. 2003. Role of the microenvironment in chronic lymphocytic leukaemia. *British Journal of Haematology* 123(3):380–388. 1.2.4, 6, A.1

Caligaris-Cappio, F., and R. Dalla-Favera, eds. 2005. *Chronic Lymphocytic Leukemia*. Springer. 1, 1.2.2, 1.2.3, A.1

Ghia, P., G. Strola, L. Granziero, M. Geuna, G. Guida, F. Sallusto, N. Ruffing, L. Montagna, P. Piccoli, M. Chilosi, and F. Caligaris-Cappio. 2002. Chronic lymphocytic leukemia B cells are endowed with the capacity to attract CD4+, CD40l+ T cells by producing CCL22. *European Journal of Immunology* 32(5):1403–1413. 1, 1.2.4, 6, A.1

Keating, M.J., N. Chiorazzi, B. Messmer, R.N. Damle, S.L. Allen, K.R. Rai, M. Ferrarini, and T.J. Kipps. 2003. Biology and treatment of chronic lymphocytic leukemia. *Hematology* 2003(1):153. 1.2.1, 1.2.3

Keller, EF, and LA Segel. 1971. Model for chemotaxis. *J Theor Biol* 30(2):225–34. 2.2

Kuznetsov, V.A., I.A. Makalkin, M.A. Taylor, and A.S. Perelson. 1994. Nonlinear dynamics of immunogenic tumors: Parameter estimation and global bifurcation analysis. *Bulletin of Mathematical Biology* 56(2):295–321. 2.1

LeVeque, R.J. 2002. *Finite Volume Methods for Hyperbolic Problems*. Cambridge University Press. 6

Martinis, M., B. Vitale, V. Zlatic, B. Dobrosevic, and K. Dodig. 2005. Mathematical model of B-cell chronic lymphocytic leukemia. *Periodicum biologorum* 107(2005):445–450. 1, 2.1

Messmer, B.T., D. Messmer, S.L. Allen, J.E. Kolitz, P. Kudalkar, D. Cesar, E.J. Murphy, P. Koduru, M. Ferrarini, S. Zupo, G. Cutrona, R.N. Damle, T. Wasil, K.R. Rai, M.K. Hellerstein, and N. Chiorazzi. 2005. In vivo measurements document the dynamic cellular kinetics of chronic lymphocytic leukemia B cells. *The Journal of Clinical Investigation* 115(3):755–764. 1, 2.1, A.1

National Cancer Institute. 2009. General information about chronic lymphocytic leukemia. Available online. URL `http://cancer.gov/cancertopics/pdq/treatment/CLL/HealthProfessional/page2`. 1

Park, C.S., and Y.S. Choi. 2005. How do follicular dendritic cells interact intimately with B cells in the germinal centre? *Immunology* 114(1):2–10. 1.1.4

Sherratt, Jonathan A. 1994. Chemotaxis and chemokinesis in eukaryotic cells: The Keller–Segel equations as an approximation to a detailed model. *Bulletin of Mathematical Biology* 56(1):129–146. 2.2, 2.2, 3.2.1, 3.2.3, A.1

Sherratt, Jonathan A., E. Helene Sage, and J.D. Murray. 1993. Chemical control of eukaryotic cell movement: A new model. *Journal of Theoretical Biology* 162(1):23–40. 2.2, 2.2, A.1

Till, Kathleen J., Mirko Zuzel, and John C. Cawley. 1999. The role of hyaluronan and interleukin 8 in the migration of chronic lymphocytic leukemia cells within lymphoreticular tissues. *Cancer Research* 59(17):4419–4426. 1.2.4, 6

Vitale, B., M. Martinis, M. Antica, B. Kusic, S. Rabatic, A. Gagro, R. Kusec, and B. Jaksic. 2003. Prolegomenon for chronic lymphocytic leukaemia. *Scandinavian Journal of Immunology* 58(6):588–600. 1, 2.1